

SECTION 7: EFFECTS OF TWO UWB SIGNALS ON THREE FEDERAL RADARS

Brent Bedford¹

7.1 Introduction

Some UWB signals appear to occupy a relatively large portion of the spectrum when compared to the spectral occupancy of the signals of conventional systems. This leads to the notion that UWB systems may need to share the same spectrum with conventional incumbents. As in the case where two conventional systems share spectrum, questions are raised about the effects of a new system sharing spectrum with an incumbent. NTIA conducted the following study to determine the levels at which a UWB signal could be present within a radar receiver.

The study involved two types of UWB signals. Both types of UWB signals consisted of pulses at a 10 MHz pulse repetition rate (PRR). Both types had the same pulse shape and amplitudes. The first signal type was dithered using pulse position modulation over 50% of its basic repetition rate. In other words, there was a basic repetition interval of 100 ns. Each pulse was delayed from 0 ns to 50 ns within each interval. The position for each pulse was determined by a uniformly distributed random number generator. The second signal type was not dithered; the pulses were generated at a constant rate. The non-dithered signal produces spectral lines which have a frequency spacing equal to the reciprocal of the pulse rate. Since the pulse rate used in this study was greater than the receiver's bandwidth, for the case of the non-dithered signal, only a single spectral line was present within the receiver's passband.

Three Federal Aviation Administration (FAA) radio receivers were involved in the testing: the Air Route Surveillance Radar (ARSR-4), the Airport Surveillance Radar (ASR-8) and the Air Traffic Control Beacon Interrogator (ATCBI-5). The ARSR-4 is a long range radar that detects targets up to 518 kilometers away. The ASR-8 assists with traffic control at airports and detects targets up to 124 kilometers away. The ATCBI-5 transmitter interrogates transponders that are located on aircraft, while its receiver detects and processes the responses from the aircraft transponders. All three of these receivers are located at the FAA Mike Monroney Aeronautical Center (MMAC) in Oklahoma City, Oklahoma.

7.2 Radiated Measurements

The radiated measurements involved radiating a signal over a line-of-sight path from the UWB source to the receiver under test. The levels, relative to the receiver's noise floor, were measured

¹The author is with the Institute for Telecommunication Sciences, National Telecommunications and Information Administration, U.S. Department of Commerce, Boulder, CO 80305.

and recorded. The results of this study will assist with determining any effects on these receivers if their spectrum is shared with UWB devices. The radars at the MMAC are good representations of radars that are operating in the field. These radars are fully functional but they are not being used to generate the critical information needed by air traffic controllers. The receivers are connected to rotating antennas that are the same as the field units. The FAA uses these radars to test new concepts before implementing the concepts on all their units and to train new personnel.

To conduct this study, the following approach was implemented. A measurement vehicle was outfitted to record the received signal level from an operating radar while the vehicle was in motion. A GPS unit was installed in the vehicle. The measurement started on the road next to the radar. The starting location was stored as a way point in the GPS receiver. The GPS receiver was set to display the distance and bearing from the vehicle to the radar. The vehicle was driven along roads that approximated radials from the transmitter. When a peak in the signal level occurred, the distance and bearing to the radar were recorded.

The results from the various runs were examined to identify the locations in which the maximum signal level was received. By reciprocity, these locations would offer the best chances for seeing any effects that the UWB transmitter would have on the receivers. The results showed that the signal level right under the radar was not the maximum level. Radar antennas typically concentrate their radiated energy into narrow beams. This is necessary for them to determine bearing and range to a target. These beams are directed into the sky to detect airborne craft. The lowest angle of interest for the beam is usually slightly above the horizon. The area under and close to the antenna is not directly illuminated by the beam, so only a moderate signal level exists. An example of this is shown in Figure 7.1. For approximately the first 1.75 horizontal divisions, the signal is relatively undefined with rapid variations. After 1.75 horizontal divisions, the spikes are well defined and vary smoothly.

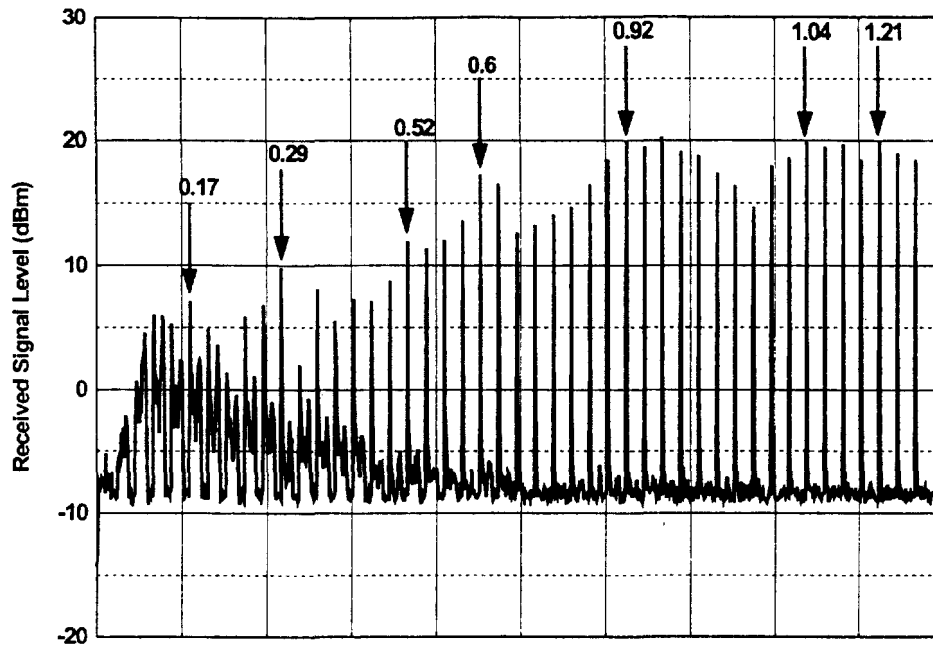


Figure 7.1. ARSR-4 signal level along a southern radial.

Foliage and buildings are other factors that influence the received signal level. When either of these obstructions enter the line-of-sight path between the vehicle and the radar, the received signal level drops rapidly and a good sample at that distance is lost. The measurements were conducted over several approximately radial paths in an attempt to get samples over a large number of distances.

Once the locations of highest signal level were known, the next part of the study took place. The Intermediate Frequency (IF) output of the radar receiver under test was connected to the spectrum analyzer. The noise level on the spectrum analyzer was noted at the expected IF frequency before connection to the IF output. All the levels were measured with the spectrum analyzer resolution bandwidth set to 1 MHz and the video bandwidth set to 10 Hz. This is the same spectrum analyzer settings that are used in a FCC Part 15 compliance measurement for frequencies above 1 GHz. The spectrum analyzer was connected to the receiver's IF output and the noise level was noted again. It was necessary for the noise coming from the IF receiver to raise the noise floor of the spectrum analyzer a perceptible amount in order for the measurements to be valid. This was the case for all of the receivers in this study.

The measurement vehicle was configured to house the UWB transmitter. A ridged horn antenna was mounted on a telescoping mast on the vehicle. While measurements were being conducted, the horn antenna was elevated above the vehicle roof to prevent reflections. For each measurement, the UWB transmitter was adjusted, by a variable attenuator, to produce an effective isotropic radiated power of -41 dBm. This level corresponds to the radiated emission limits found in FCC Part 15.209 for frequencies above 1 GHz.

The measurement vehicle was parked near some of the locations of highest signal level as well as a few others. It usually was not possible to pull off the road right where a peak occurred. The horn antenna was raised and pointed at the radar under test and the UWB transmitter was activated. The radar transmitter was then turned off and its antenna was manually pointed in the azimuth of the vehicle. The antenna was swung through many degrees to find the peak delta marker value, which was recorded. The delta marker value consists of setting a reference level with the UWB transmitter off, then measuring the decibel increase in the level with the UWB transmitter on. Various attenuator settings were tried. The attenuator settings and the resulting delta marker values were recorded.

In addition to the UWB transmitter measurements, a few incidental radiators were activated, with line-of-sight paths to the radars, at the above sites. The delta marker values due to these devices were recorded. This shows a comparison between UWB sources and incidental radiators.

7.2.1 ARSR-4 Radiated Measurements

The ARSR-4 receiver frequency was 1241.47 MHz. The PRR for the non-dithered UWB signal had to be adjusted to put a spectral line within the passband of the receiver. It was calculated that if the PRR was increased by 10.01 kHz, this would put a spectral line at 1241.241 MHz. This new PRR was used for this radar.

The vehicle was driven along two paths. One path was along a southern radial that started at the radar. The received signal level along this path is shown in Figure 7.1. The graph is labeled with the distances from the radar in kilometers where the peaks occurred. The second path was on a southern path that started 0.64 kilometers west of the radar. The received signal level along this path is shown in Figure 7.2. On this graph, there is a gap in time, because the vehicle was stopped and some time passed before the recording resumed. Although the vehicle was driven at a constant speed and in most cases distances can be interpolated between the marks on the graph, one should not interpolate across the gap in time.

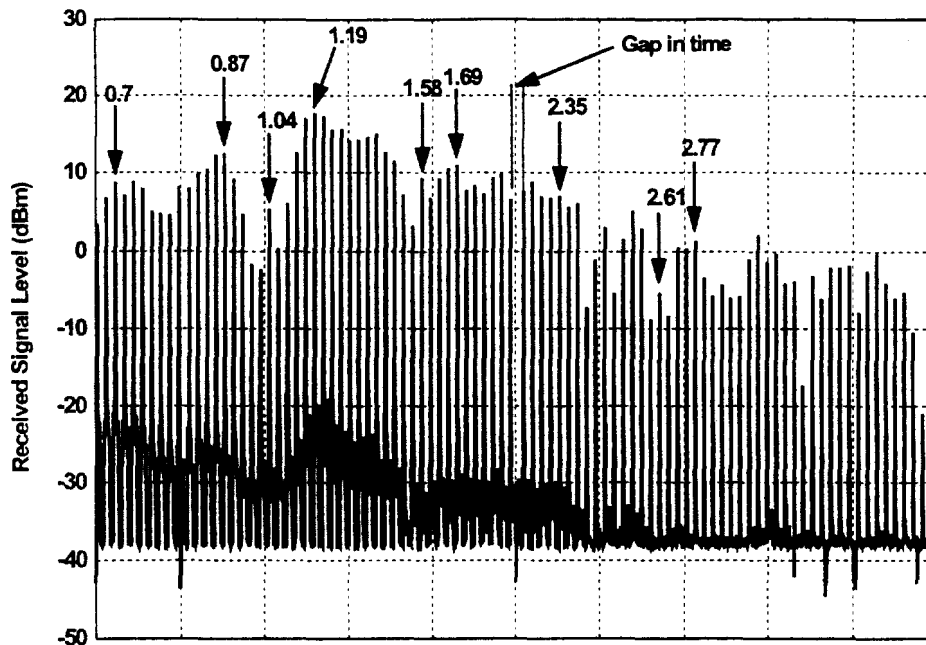


Figure 7.2 ARSR-4 signal level along a southern path.

Next, the vehicle was driven to three sites where measurements were performed. The first site was 1.26 kilometers from the radar at a bearing of 178 degrees. For a 10 MHz PRR dithered signal, radiated at the FCC Part 15.209 radiated emission limit, the delta marker value was 9 dB. Attenuating the UWB transmitter output by 6 dB brought the delta marker value down to 6 dB. Attenuating the UWB transmitter output by 12 dB brought the delta marker value down to 2 dB. Attenuating the UWB transmitter output by 15 dB brought the delta marker value down to 1 dB. For the non-dithered signal, radiated at the FCC Part 15.209 radiated emission limit, the delta marker value was 0 dB. In this case, the UWB signal did not affect the noise floor. An electric drill and an electric shaver were turned on to see if their radiation could be observed at the receiver's IF. The electric shaver produced asynchronous spikes 10 to 15 dB above the noise floor but this did not affect the noise floor. This is shown in Figure 7.3. The electric drill did not affect the noise floor.

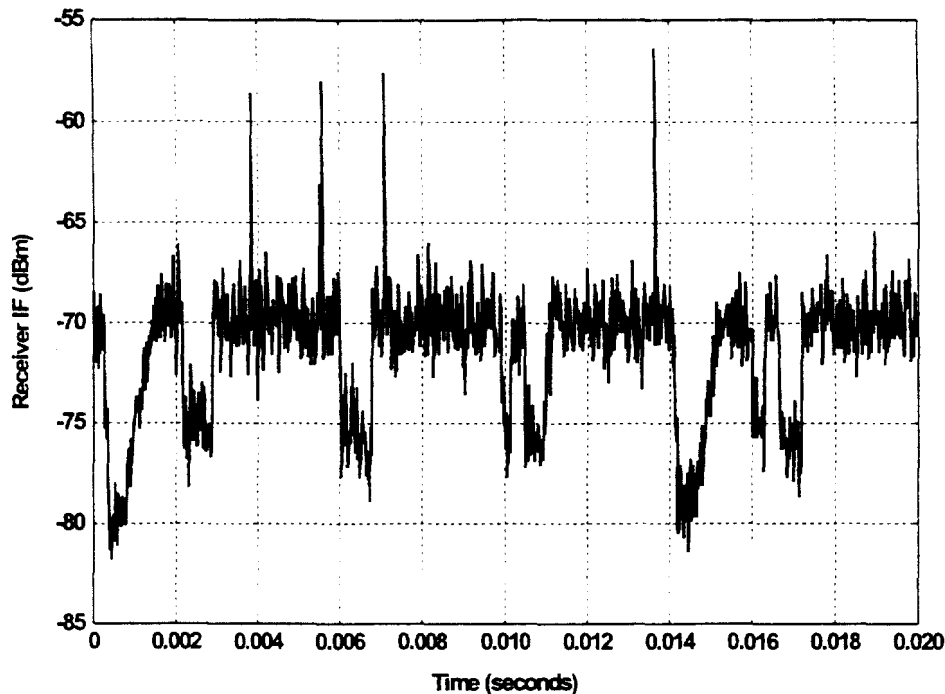


Figure 7.3. Asynchronous spikes produced by the electric shaver.

The second site was 2.08 kilometers from the radar at a bearing of 199 degrees. For a 10 MHz PRR dithered signal, radiated at the FCC Part 15.209 radiated emission limit, the delta marker value was 11 dB. Attenuating the UWB transmitter output by 6 dB brought the delta marker value down to 8 dB. Attenuating the UWB transmitter output by 12 dB brought the delta marker value down to 4 dB. Attenuating the UWB transmitter output by 18 dB brought the delta marker value down to 2 dB. For the non-dithered signal, radiated at the FCC Part 15.209 radiated emission limit, the delta marker value was 0 dB. In this case, the UWB signal did not affect the noise floor. An electric drill and an electric shaver were turned on to see if their radiation could be observed at the receiver's IF. Neither item affected the noise floor.

The third site was 3.17 kilometers from the radar at a bearing of 53 degrees. For a 10 MHz PRR dithered signal, radiated at the FCC Part 15.209 radiated emission limit, the delta marker value was 8 dB. Attenuating the UWB transmitter output by 6 dB brought the delta marker value down to 5 dB. Attenuating the UWB transmitter output by 12 dB brought the delta marker value down to 2 dB. Attenuating the UWB transmitter output by 15 dB brought the delta marker value down to 1 dB. For the non-dithered signal, radiated at the FCC Part 15.209 radiated emission limit, the delta marker value was 0 dB. In this case, the UWB signal did not affect the noise floor. An electric drill and an electric shaver were turned on to see if their radiation could be observed at the receiver's IF. Neither item affected the noise floor.

For a dithered UWB signal, radiated at the FCC Part 15.209 radiated emission limit, the maximum delta marker value was 11 dB. For a non-dithered UWB signal, radiated at the FCC

Part 15.209 radiated emission limit, the maximum delta marker value was 0 dB.

7.2.2 ASR-8 Radiated Measurements

To find the locations of highest signal level, the vehicle was driven along three paths. One path started at the radar, went west for 0.22 kilometers, then went north. The received signal level along this path is shown in Figure 7.4. The second path was on a northern radial that started approximately 0.48 kilometers northeast of the radar. The received signal level along this path is shown in Figure 7.5. The third path was a northward extension of the first path. This path started 0.78 kilometers northwest of the radar and went north. The received signal level along this path is shown in Figure 7.6. On this graph, there is a gap in time, because the vehicle was stopped and some time passed before the recording resumed. Although the vehicle was driven at a constant speed and in most cases, distances can be interpolated between the marks on the graph, one should not interpolate across the gap in time.

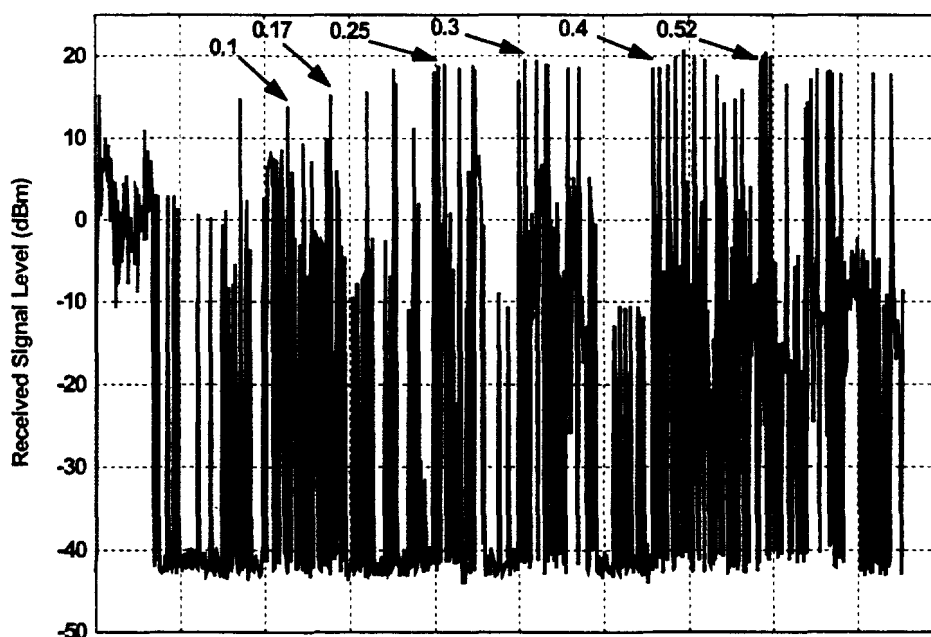


Figure 7.4. ASR-8 signal level along a mostly northern path.

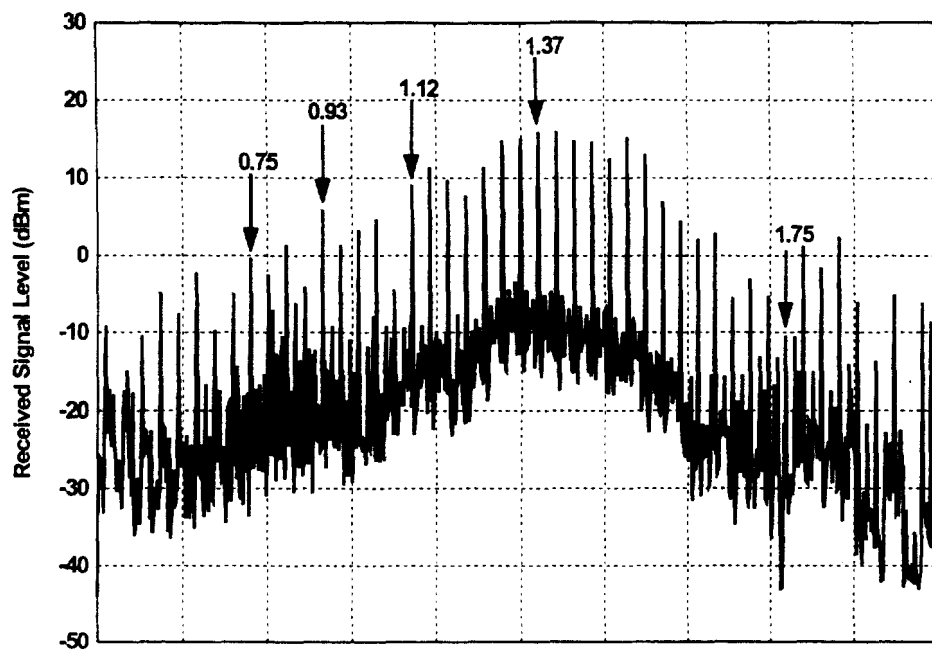


Figure 7.5. ASR-8 signal level along a northern radial.

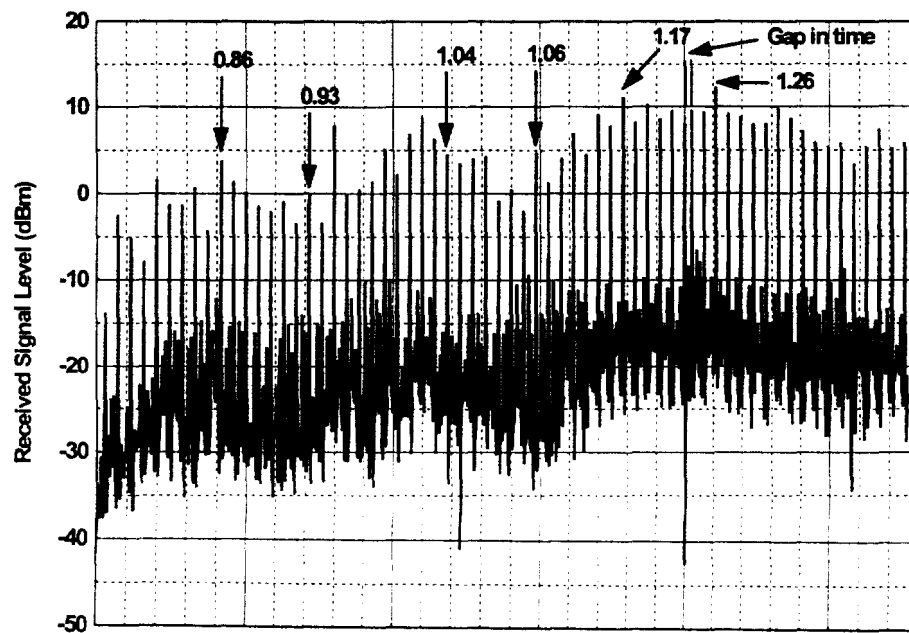


Figure 7.6. ASR-8 signal level along a northern extension of figure 7.4.

Next, the vehicle was driven to two sites where measurements were performed. The two sites were located as close to a recorded signal peak as possible. The first site was 0.4 kilometers from the radar at a bearing of 326 degrees. For a 10 MHz PRR dithered signal, radiated at the FCC Part 15.209 radiated emission limit, the delta marker value was 6 dB. Attenuating the UWB transmitter output by 3 dB brought the delta marker value down to 3 dB. For the non-dithered signal, radiated at the FCC Part 15.209 radiated emission limit, the delta marker value was 5 dB. Attenuating the UWB transmitter output by 3 dB brought the delta marker value down to 2 dB. An electric drill, electric hair dryer and an electric shaver were turned on to see if their radiation could be observed at the receiver's IF. These items did not affect the noise floor.

The second site was 1.41 kilometers from the radar at a bearing of 11 degrees. For a 10 MHz PRR dithered signal, radiated at the FCC Part 15.209 radiated emission limit, the delta marker value was 1 dB. For the non-dithered signal, radiated at the FCC Part 15.209 radiated emission limit, the delta marker value was 3 dB. Attenuating the UWB transmitter output by 2 dB brought the delta marker value down to 2 dB. An electric drill, electric hair dryer and an electric shaver were turned on to see if their radiation could be observed at the receiver's IF. These items did not affect the noise floor.

For a dithered UWB signal, radiated at the FCC Part 15.209 radiated emission limit, the maximum delta marker value was 6 dB. For a non-dithered UWB signal, radiated at the FCC Part 15.209 radiated emission limit, the maximum delta marker value was 5 dB.

7.2.3 ATCBI-5 Radiated Measurements

This radar at this location is mounted on top of a 30.5 meter tower. Because the typical ASR beacon installation is not this high, these measurements may give rather optimistic results. If the UWB signal was seen by this configuration, then the typical configuration would probably see the signal at a higher level.

The vehicle was driven to two sites where measurements were performed. The first site was 1.26 kilometers from the radar at a bearing of 178 degrees. For a 10 MHz PRR dithered signal, radiated at the FCC Part 15.209 radiated emission limit, the delta marker value was 0 dB. For the non-dithered signal, radiated at the FCC Part 15.209 radiated emission limit, the delta marker value was 0 dB. An electric drill and an electric shaver were turned on to see if their radiation could be observed at the receiver's IF. These items did not affect the noise floor.

The second site was 0.5 kilometers from the radar at a bearing of 178 degrees. For a 10 MHz PRR dithered signal, radiated at the FCC Part 15.209 radiated emission limit, the delta marker value was 1 dB. For the non-dithered signal, radiated at the FCC Part 15.209 radiated emission limit, the delta marker value was 0.6 dB. An electric drill and an electric shaver were turned on to see if their radiation could be observed at the receiver's IF. These items did not affect the noise floor.

For a dithered UWB signal, radiated at the FCC Part 15.209 radiated emission limit, the maximum delta marker value was 1 dB. For a non-dithered UWB signal, radiated at the FCC Part 15.209 radiated emission limit, the maximum delta marker value was 0.6 dB.

While the vehicle was parked 15.2 meters from this radar, an electric drill and an electric shaver were turned on to see if their radiation could be observed at the receiver's IF. These items did not affect the noise floor.

7.3 Summary

It is instructive to gather the results into tables for examination. Table 7.1 contains the delta marker values for the dithered UWB signal. Table 7.2 contains the delta marker values for the non-dithered UWB signal. All of the values correspond to the cases where the UWB signal is radiated at the FCC Part 15.209 radiated emission limit. The results indicate that all three radars experience a noticeable effect for at least one and in some cases, both types of UWB signals that were generated in this study. The ARSR-4 presented an interesting case in two ways. Within the constraints of three site testing, Table 7.1 shows a relatively large effect with a dithered signal and Table 7.2 shows no effect with a non-dithered signal.

Table 7.1. Delta Marker Values in Decibels for the Dithered UWB Signal.

Radar	First Site	Second Site	Third Site
ARSR-4	9	11	8
ASR-8	6	1	
ATCBI-5	0	1	

Table 7.2. Delta Marker Values in Decibels for the Non-Dithered UWB Signal.

Radar	First Site	Second Site	Third Site
ARSR-4	0	0	0
ASR-8	5	3	
ATCBI-5	0	.6	

8. MEASUREMENT SUMMARY AND CONCLUSIONS

Robert .J. Matheson¹

8.1 Introduction

This section contains a summary of the measurements made on various UWB devices using the measurement techniques described in Sections 5 and 6. The data presented in this section have been selected from the total measurement set made on each UWB device; additional measurement data for each device is included in Appendix D.

Measurements from six devices are included.

Device A	Section 8.3.1, Appendix D-A
Device B	Section 8.3.2, Appendix D-B
Device C	Section 8.3.3, Appendix D-C
Device D	Section 8.3.4, Appendix D-D
Device E	Section 8.3.5, Appendix D-E
Electric drill	Section 8.3.6, Appendix D-F

8.2 Examples for Detailed Analysis

This section describes the selected measured data in detail, using examples from Devices A, B, and D. It is expected that the reader will apply the explanations to corresponding data from the remainder of the UWB devices, as appropriate. Data for each device will be presented in the same order to facilitate locating data and comparing results between different devices

8.2.1. Device Description

This is a short description of the UWB technology employed. ITS is making no claims that the UWB device works as intended or as described. In most cases, ITS did not functionally test the UWB device performance in any way (except to ascertain that the UWB transmitter was apparently functioning), and consequently ITS is unaware of whether a specific UWB device achieves any of its intended or claimed functional performance objectives.

¹The author is with the Institute for Telecommunication Sciences, National Telecommunications and Information Administration, U.S. Department of Commerce, Boulder, Colorado 80305

Device A uses a 10-kHz pulse repetition rate (PRR), apparently not gated, dithered, or modulated. ITS had no information on the operational aspects of this device (e.g., whether there was any adaptive modification of transmitter modes depending on device location), and testing proceeded on the assumption that the on-off switch was the only significant test variable.

8.2.2. Full-Bandwidth Pulse Shape

Figure 8.1 is an example of a full-bandwidth pulse shape measurement, as described in Section 5. Major objectives of this measurement include understanding full bandwidth pulse shapes, evaluating the possible utility of various pulse-width models for engineering and regulatory purposes (especially to relate pulse shape to the emission spectrum), and furnishing raw data for fast Fourier transform (FFT) computations of emission spectra.

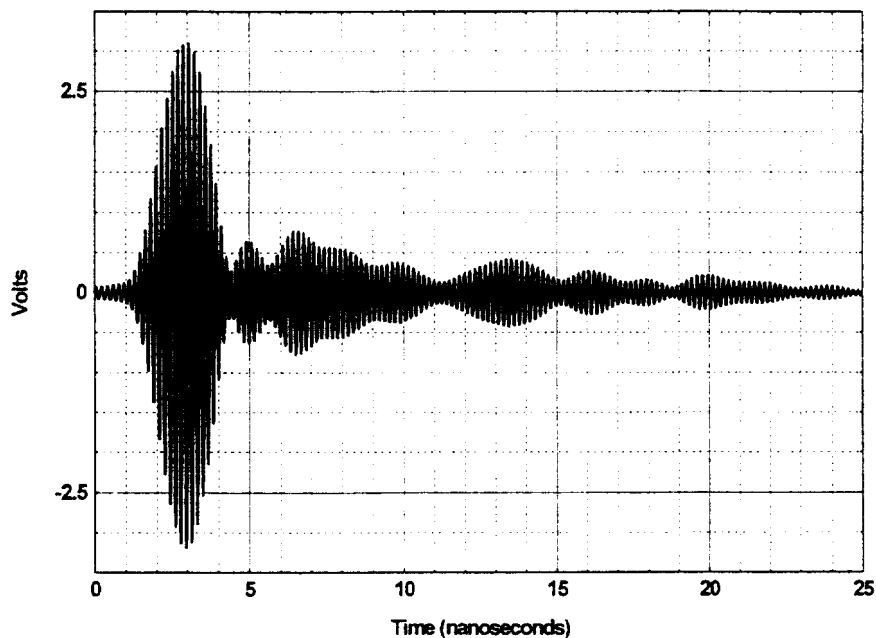


Figure 8.1. Device A full bandwidth pulse shape.

Depending on the UWB device, the full bandwidth pulse shape measurements were made on a conducted basis and/or a radiated basis at a distance of 1 meter. Conducted measurements were calibrated in dBm; radiated measurements were calibrated in voltage available at the terminals of a ridged horn or TEM horn antenna at a distance of 1 m. For the radiated measurements, the effects of the measurement antenna frequency-dependent gain and delay on the pulse shape have not been corrected, though techniques to provide a calibration in absolute field-strength are still being investigated. This process would involve performing an FFT of the uncorrected pulse, correcting the resulting spectrum with frequency-dependent antenna delay and gain factors, and performing an inverse FFT on the corrected spectrum to obtain a corrected pulse shape.

The Device A full bandwidth pulse shape in Figure 8.1 is relatively complex, involving multiple lobes and many crossings of the zero-axis. A complex waveform like this is typical of UWB signals that have been filtered with relatively high-Q resonant circuits to provide a signal limited to a well-controlled RF bandpass. Other UWB devices (e.g., Device E) may have a much simpler pulse shape with only a few zero-crossings.

8.2.3. FFT Emission Spectrum

Figure 8.2 is an example of an emission spectrum calculated via FFTs from the full-bandwidth pulse shape in the previous figure. Device A's full bandwidth pulse shape was measured in the conducted mode, so the spectrum calculated via FFTs was calibrated in peak dBm in a specific bandwidth = Δf . In this case, a Δf bandwidth of 16.7 MHz was used. For large bandwidths, the calculated peak dBm will change according to a $20 \log_{10} B$ rule.

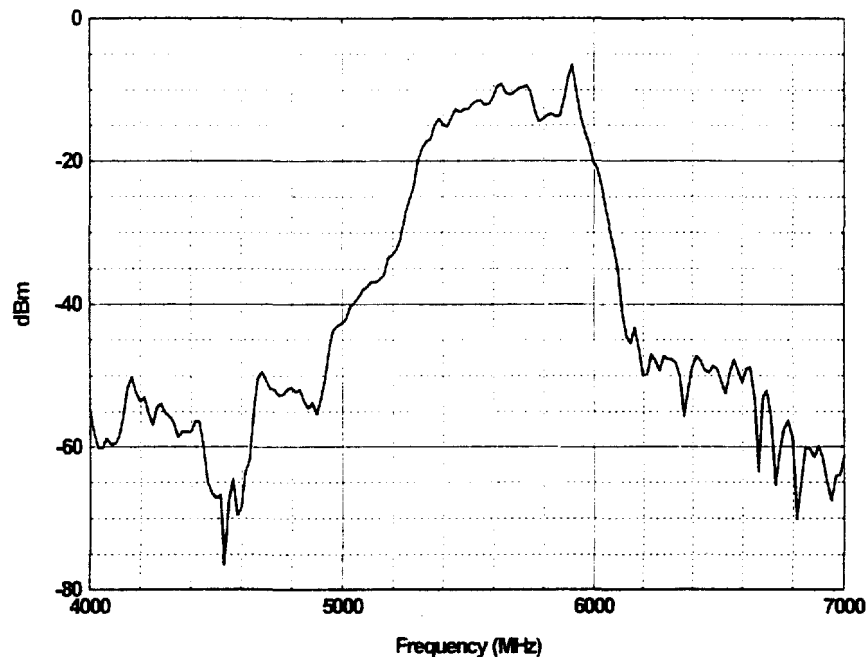


Figure 8.2. Device A conducted FFT spectrum, $\Delta f = 16.7\text{MHz}$.

Most of the UWB devices were measured in the radiated mode at a distance of 1 meter. In the radiated pulse shape measurements, the pulse shape was not corrected for the effects of the frequency-dependent receiving antenna gain. However, the spectrum calculated from the pulse shape via FFTs is corrected for antenna gain and plotted as field strength at 1 meter. The field strength values are based on peak power in a given computational bandwidth, Δf , and plotted in $\text{dB}\mu\text{V/m}$. The peak field strength can be directly compared to the spectrum analyzer measurements by using an appropriate bandwidth conversion factor (e.g., $20 \log_{10} B$ for wider bandwidths where the UWB pulses are independently resolved). The FFT is based on the

emission from a single pulse. Therefore, it contains none of the spectrum fine structure caused by a train of impulses and the associated pulse train modulation techniques.

Major objectives for FFT calculation of emission spectra include a comparison with spectrum analyzer measurements. Close agreement between FFT and measured spectra ensures confidence in the accuracy of the full-bandwidth pulse shape measurements and the adequacy of narrowband spectrum analyzer measurements in determining the RF envelope of UWB emissions. Since the Device A full bandwidth pulse shape (and the corresponding FFT spectra) was measured in the conducted mode, while the spectrum analyzer measurements in the following sections were made in the radiated mode, no direct quantitative comparison of the full bandwidth measurements and the spectrum analyzer measurements is possible. A full set of radiated measurements were made with many of the other UWB devices, however, and these show good quantitative comparison between the full bandwidth data and the spectrum analyzer data. On a qualitative basis, the Device A conducted FFT spectrum shows the same concentration of energy in the 5300-6100 MHz region shown in the radiated spectrum analyzer measurements described next.

8.2.4. Narrowband Peak Emission Spectra

Figure 8.3 contains a series of emission spectra measured at a distance of 1 m with a spectrum analyzer using a peak detector and bandwidths of 10 kHz to 3 MHz, as described in Section 6.4.2. This data is calibrated using two scales: The left-hand scale is in dBm, referenced to the antenna terminals of an imaginary antenna having a constant aperture equivalent to what a 5.9 dBi antenna would have at 1 GHz. This calibration removes the effects of a frequency-dependent receiving antenna aperture (unlike the full-bandwidth pulse measurements), leaving the dBm value unchanged at 1 GHz. The right-hand scale is in dB μ V/m at a distance of 1 m. The details of these calibrations can be found in Appendix C.

Major objectives for these measurements include development of techniques for UWB spectrum measurements using commercial off-the-shelf (COTS) equipment, investigation of the relative utility of -10-dB and -20-dB and mid-band frequency points on the UWB spectra, peak detector bandwidth correction factors, investigation of preferred spectrum measurement bandwidths for various regulatory and modeling purposes, and comparison with spectra derived by FFT processing of full bandwidth pulse shapes. Successful comparison between the FFT-derived emission spectra and spectrum analyzer measurements would strongly suggest that spectrum analyzer measurements in a narrower bandwidth are accurate and adequate for purposes of describing the overall UWB emission spectrum, along with the -10-dB and -20-dB frequency points.

If the measurement system bandwidth is sufficiently greater than the UWB device PRR, the UWB impulses are resolved in the measurement system IF as independent, non-overlapping pulses – also called "impulsive" behavior. The peak value of these pulses is expected to depend on the measurement bandwidth, B, according to a $20 \log_{10} B$ rule. This would result in approximate 10-dB differences between successively larger measurement bandwidths, when

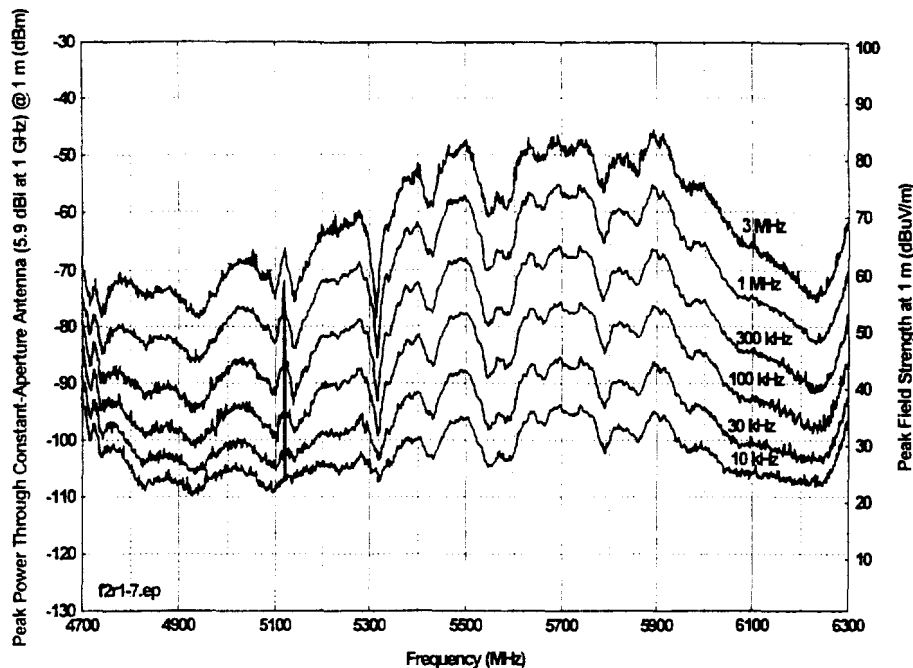


Figure 8.3. Device A measured spectra as a function of bandwidth.

those bandwidths increase in a 1, 3, 10 progression. In this example, the 10-kHz PRR of Device A causes the peak signal to appear impulsive for all measurement bandwidths greater than 10 kHz (i.e. all of the bandwidths measured in Figure 8.3).

If the measurement bandwidth is less than the UWB PRR, the UWB energy is stretched out in time in the receiver IF such that successive UWB pulses overlap, causing the appearance of a more-or-less continuous signal. Depending on the timing between successive UWB impulses, the IF signal can appear like a continuous wave (CW) signal, or Gaussian noise, or other modulations. Signals that appear noise-like are expected to follow a $10 \log_{10} B$ rule. This would result in approximate 5-dB increases between successively larger measurement bandwidths, when the bandwidths follow a 1, 3, 10 progression. Signals that have a CW appearance do not change in amplitude as the measurement bandwidth is increased. In this example, since no emission spectrum measurements were made with bandwidths less than 10 kHz, there was no opportunity to observe the behavior of signals from Device A in the noise-like or CW region.

Most of the energy in this spectrum is contained in the 5300-6100 MHz range. These spectra have numerous irregular lobes that were about 250 MHz wide, with 10-20 dB nulls between them. Detailed measurements showing UWB signal behavior as a function of higher spectrum resolution, bandwidth, and/or time, as described in the remainder of this section, were made near 5700 MHz. The measurements near 5700 MHz show an impulsive behavior (10 dB between successive measurement bandwidths). Measurements made near 4800 MHz or 6200 MHz tend to show 5-dB differences between successive bandwidths. This was probably because the UWB peak signals were not sufficiently above the measurement system noise levels near these

frequencies, and the measurements were substantially affected by system noise (5-dB difference between successive detector bandwidths).

8.2.5. Spectrum Fine Structure

The details of the spectrum fine structure are a result of the techniques used for dithering or modulating the pulse train. In general, various measurements of the detailed spectrum fine-structure were attempted for all UWB devices, but these measurements sometimes provided inconclusive results that were not included in this collection of significant measurement results. The purpose of these measurements was to gain information on PRR and modulation details so that later measurements of APDs and detector values could be understood more completely.

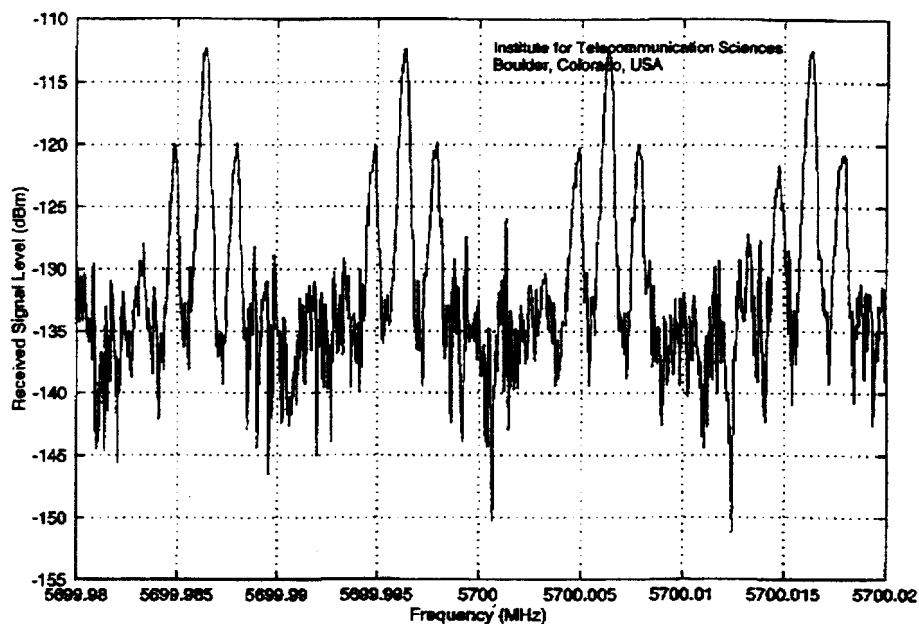


Figure 8.4. Device A spectrum fine structure (5700 MHz).

Measurements of spectrum fine-structure may reveal unexpected details like the repetition frequency of the sequence used to dither the impulse train, etc. Specifically, non-dithered pulse trains will show discrete spectral lines at harmonics of the PRR. When the basic PRR is dithered with a sequence that repeats at a certain rate, discrete spectral lines will appear separated by that rate (frequency). The relative amounts of energy in the spectral lines caused by the dither sequence, the spectral lines caused by the PRR, and the continuous spectral background are determined by the modulation and dithering details.

Device A (Figure 8.4) showed major spectral lines at a 10-kHz spacing, as expected from the 10-kHz PRR that was measured in the time domain. A closer examination showed the additional fine structure of distinct spectral lines on either side of the main lines about 1700 Hz away. The cause of these sidebands is not known.

8.2.6. Bandwidth Progression Stairstep Measurements

This measurement shows the values of peak detector readings made with a range of measurement bandwidths (100 Hz - 3 MHz). Specifically, it shows that the UWB device PRR causes impulsive behavior (10-dB steps between successive measurement bandwidths) for bandwidths greater than the PRR. For bandwidths less than the PRR this graph will show noise-like (5-dB steps between successive bandwidths), CW-like (constant values independent of bandwidth), and various other behaviors.

Figure 8.5 shows the peak signal level bandwidth progression measurements for Device A (PRR = 10 kHz), showing 10-dB spacing for bandwidths greater than 10 kHz. The apparent departure from 5-dB spacing for some of the narrower measurement bandwidths is caused by: 1) the details of the dithering technique, 2) the measurement frequency, and 3) the lower number of independent samples (which limits the ability of the peak detector to reach statistically valid peak

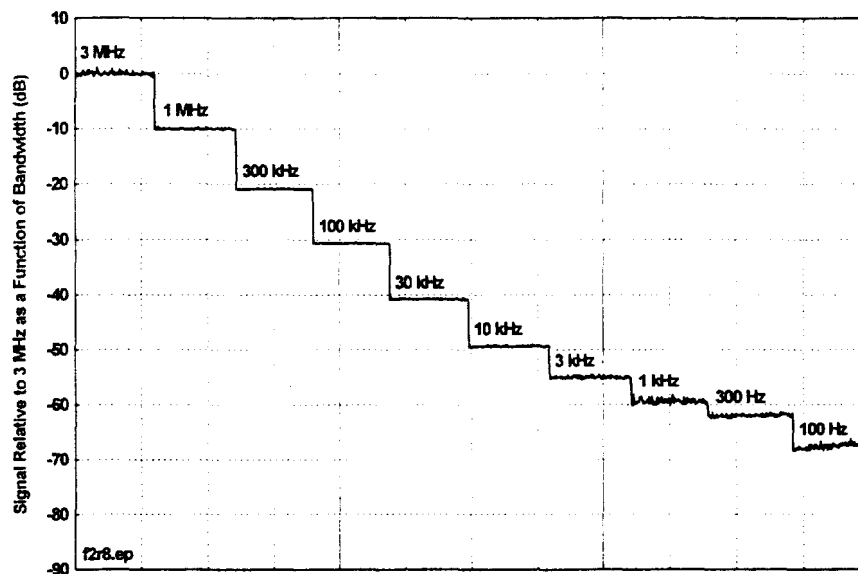


Figure 8.5. Device A, peak signal bandwidth progression stairstep .

values). This last factor is apparently not present in the Device A measurements, but it can be seen clearly in the measurements of some of the other devices (e.g. Device B, Figures 8.20 and 8.21). It is present in those cases because the rate at which independent samples occur is proportional to the measurement bandwidth, and the decreased bandwidth results in fewer independent samples during the fixed time period of these samples. This accounts for the jagged appearance of the narrowest bandwidths, where many of the time samples failed to contain any of the statistically rarer peaks that are 8-10 dB above the average values. For these cases, the 5-dB rule appears to be maintained more closely if one considers the peak value seen within the whole stair "step." Using the whole "step" has the effect of increasing the number of independent samples for the lowest bandwidths, partially correcting the problem of too few samples.

8.2.7. Gating, PRR, and Modulation

These observations are intended to show the occurrence of patterns of pulses, as measured in the time domain at a single frequency. The purpose of these measurements was to help gain detailed information on PRR and modulation so that later measurements of APDs and detector values could be understood more completely. Depending on the features employed in a specific UWB device, these measurements could show the basic PRR (Figure 8.6), the pattern of gated pulse bursts (Figure 8.23), or the modulation method used to add dithering or data to the pulse trains (Figure 8.26). Such modulation methods could include on-off modulation of individual pulses, fixed or variable pulse delays referenced to an absolute time base, or fixed or variable pulse delays referenced to the preceding pulse. These measurements can be gathered under a wide range of bandwidths, time scales, and detector types, as needed to best show the details of the significant features.

Figure 8.6 shows the appearance of the Device B as a function of time, as seen using a wideband RF detector with logarithmic compression. This figure shows a 100-kHz PRR gated pulse train, without apparent dithering or other modulation.

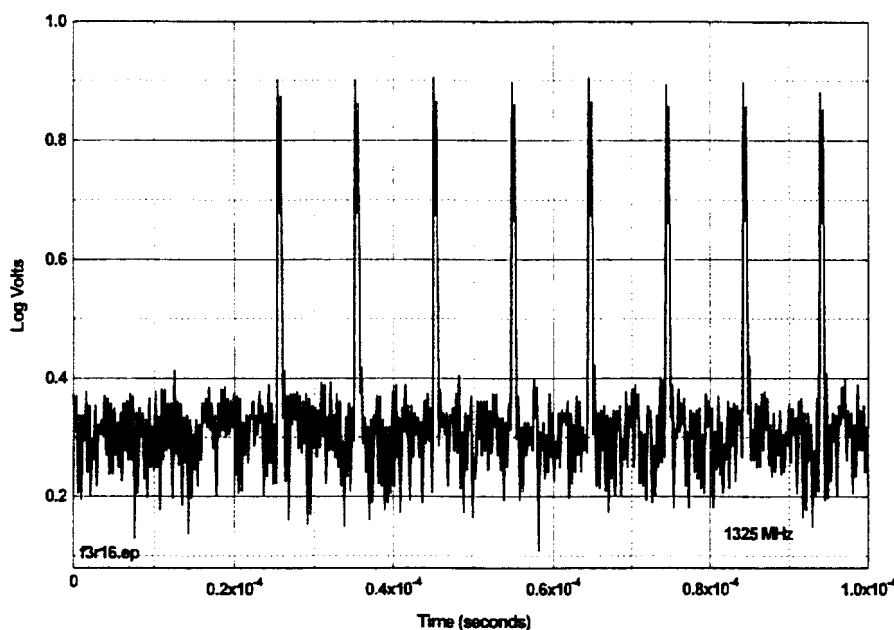


Figure 8.6. Device B, pulse train PRR, 16 kBit/second mode, external detector.

In addition to dithering (used to make UWB emission spectra look more noise-like) and modulation (employed to provide for transmission of data), some UWB systems also employ gating. A gated system employs a programmed set of periods where the UWB transmitter is turned off or on for a period of many UWB pulses. For example, a UWB system might transmit a gated burst of data lasting 10 ms, followed by a 40-ms period where no pulses are transmitted.

These so-called "gated" modes are different from data encoding techniques, where individual pulses are turned off or on to encode a digital message.

8.2.8. Amplitude Probability Distribution (APD)

The APD contains information on the percentage of time the envelope of UWB signals in a specific IF bandwidth exceeds various amplitudes. A more complete description of APDs is included in Appendix A. Figure 8.7 contains APDs from Device D, 1-MHz PRR, 100% gating (i.e., transmitting continuously). These APDs were measured in bandwidths between 10 kHz and 20 MHz at a single center frequency near the frequency of maximum UWB spectral power. With some devices, two sets of APDs were measured to distinguish between different signal fine structures seen at different frequencies. Some UWB devices measured earlier in the measurement program did not include the 10-MHz and 20-MHz bandwidth measurements, as this capability was not yet available to us.

Since the APD will change substantially as a function of measurement bandwidth (or in victim receivers having various bandwidths), the graph contains a family of APDs measured in bandwidths between 10 kHz and 3 MHz, and sometimes including 10-MHz and 20-MHz bandwidths. The APD provides a conceptual technique for understanding how various UWB signals will appear within victim receivers of various bandwidths. In particular, since the raw bit error rate of a victim receiver is closely related to the probability that the interfering UWB signal will exceed the amplitude of the desired signal, the APD provides a tool to relate UWB characteristics to the interference caused to various victim systems. (Note that many modern systems employ a variety of error correction techniques that are intended to correct most raw bit errors, so the number of errors presented to the system user may be related to the APD in more complex ways.)

The APD graph is plotted in power (dBm) versus the percentage of time (or probability) that the signal envelope will exceed a specified level. The percentage-of-time scale is weighted as $0.5 \log_{10}(-\ln P(A > a))$, as described in Appendix A. This particular weighting function has two important consequences. First, the envelope of Gaussian noise (including receiver noise) plots as a straight line, making it easy to recognize when UWB signals act in a non-Gaussian manner. Second, these APD graphs never reach 0% or 100%, but only approach these percentages. This reflects the real world circumstance that the maximum and minimum peak amplitudes of many phenomena (including Gaussian noise) are dependent on the total number of independent measurements included in the sample.

In the APD graph, the individual APDs are labeled by IF measurement bandwidth. The amplitude (power) scale is in dBm, referred to the output terminals of the measurement antenna, which was located 1 m from the UWB source. The gain of the ridged-horn measurement antenna was between 5 dBi and 10 dBi, depending on the measurement frequency. Although the APD calibration could have been converted to field strength, the primary object of the APD

measurements and analysis was to show the relative behavior of UWB signals as a function of measurement bandwidth (where absolute field strength calibration was less important).

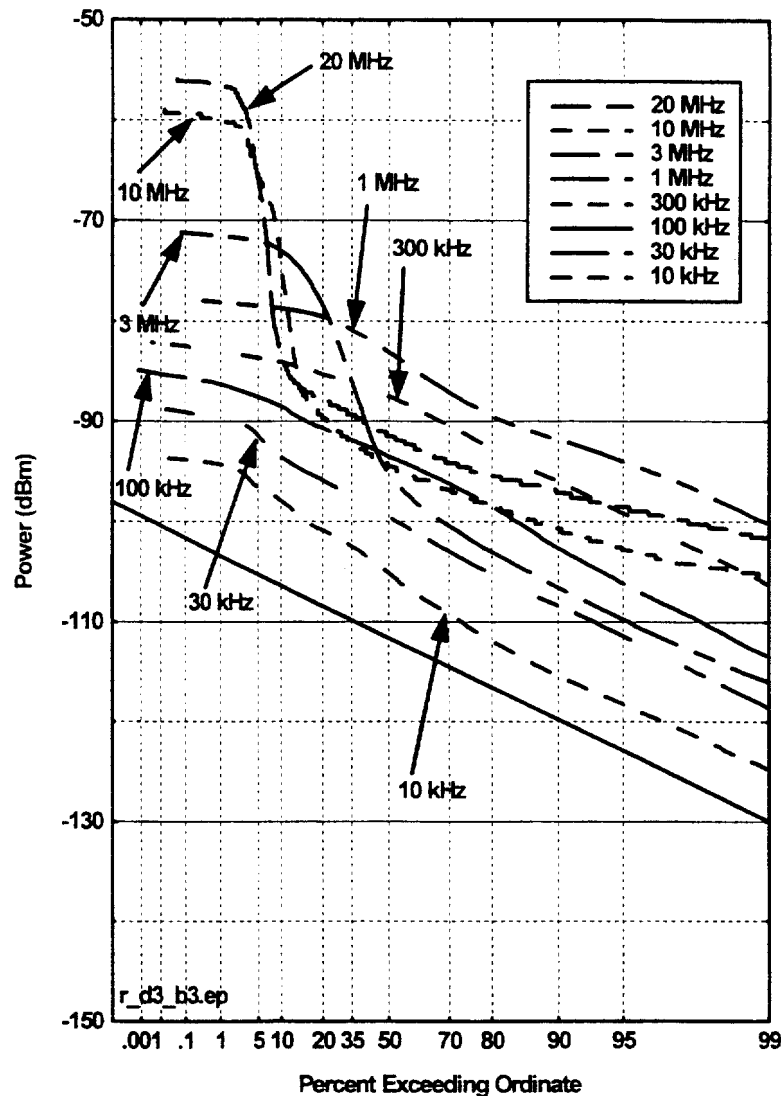


Figure 8.7 Device D APDs, 1-MHz PRR, 100% gating.

Most APDs show two distinct patterns, depending on the relationship of the measurement bandwidth to the PRR. For measurement bandwidths greater than the PRR (bandwidths of 3 MHz and above for Device D, PRR = 1 MHz), the UWB signals look impulsive. This means that the individual UWB RF impulses are converted to independent pulses within the receiver IF bandwidth. The peak amplitude of these IF pulses varies as $20 \log_{10} B$, and the duration of these pulses is approximately $1/B$. For example, in the 10-MHz bandwidth, each pulse will last approximately $0.1 \mu\text{s}$. With a PRR of 1 MHz, the total duration of these pulses adds up to a total of 0.1 s each second. This is a total pulse duration equal to about 10% of the total time, matching the approximate 10% "plateau" on the 10-MHz APD in Figure 8.7.

The peak amplitude of the plateau is expected to vary according to a $20 \log_{10} B$ rule for independent pulses. Thus, the 20-MHz APD should have a peak value 16.5 dB greater than the 3-MHz APD – very close to the difference in Figure 8.7.

As shown in the graph, the Device D pulse was present in the 20-MHz bandwidth about 5% of the total time. During the 95% of the time that the Device D pulse was not present in the measurement receiver, the only "signal" present in the measurement receiver was receiver system Gaussian noise. Thus, the remainder of the APD (after the impulsive signals have been subtracted) is only system noise. In the example, the 20-MHz APD tends to match a straight line drawn on the graph corresponding to Gaussian noise over the percentage ranges between about 20% and 80%. This straight line corresponds to a 20-MHz receiver bandwidth with a noise figure of 10 dB. The APD of system noise corresponding to other bandwidths and noise figures would be represented by a straight line with an identical slope, but offset vertically and intercepting the 37% value at Noise (dBm) = $NF + 10 \log_{10} B(\text{Hz}) - 174$, where NF is the measurement system noise figure in dB.

The departure of the measured APDs from the expected Gaussian noise straight line (the 80-99% range on the 20-MHz APD, and various amounts on other curves) is not completely resolved, but it is probably due to insufficient video bandwidth in the measurement system that was assembled to make the 10-MHz and 20-MHz bandwidth measurements. As expected, the departure-from-ideal-response was greater for the wider bandwidths.

Within measurement bandwidths equal to or less than the UWB PRR (1-MHz and less, in this example), the UWB energy does not appear as independent pulses. In this "non-impulsive" mode, the energy from successive UWB pulses is sufficiently stretched out in time by the IF bandwidth filter that the "pulses" overlap. Depending on the timing between pulses, the overlapping pulses can constructively or destructively interfere in the receiver IF bandwidth. This process can produce various results, including a series of discrete spectral lines at the harmonics of a uniform undithered PRR, or a continuum of energy resembling Gaussian noise for modulated or dithered UWB pulse trains. The use of a repeated binary sequence to dither the pulse train can produce discrete close-spaced spectral lines at frequencies related to the repetition rate for the whole sequence.

Although some dithering or modulation techniques may produce signals that appear like Gaussian noise in narrow bandwidths, this apparent Gaussian noise is different in origin from the Gaussian noise that is present in the wider bandwidth impulsive modes and in gated modes. In the narrowband mode (bandwidths less than the PRR) the energy from ungated UWB impulses is continually present in a narrow IF bandwidth, and the measured signal (often a signal with Gaussian characteristics) comes from the UWB energy. In wideband and gated modes, there are time intervals where no UWB energy is present, and measurement system (Gaussian) noise appears whenever the UWB energy is absent. Therefore, although the APDs measured in these two cases may both appear like Gaussian noise, it is important to note that for gated signals or wide measurement bandwidths the low amplitude Gaussian portion of the APD is not caused by

the UWB signal. In the case of the Device D example, the amplitude of the Gaussian noise in the 30-kHz APD is about 17 dB higher than would have been calculated on the basis of system noise figure and bandwidth.

8.2.9. Detector Summary

While the complete APD data set may give good insights on how specific UWB devices will interact with specific victim receivers, a specification for computing a single numerical value from any APD may be desirable for comparing UWB emissions with regulatory limits. APDs can be processed to give numerical values for detector functions (called "statistics" in Appendix A) like peak, RMS, average voltage, average logarithm, median, etc. The specific intent of this section is to explain the numeric values produced by various detectors and measurement bandwidths, based on the particular characteristics of UWB signals. These results are intended to give information on which detector functions and bandwidths are most suited for specifying Part 15 limits, rather than to suggest specific numerical values for these limits.

Since the APD contains only first-order statistics, presumably any detector function that can be derived from first-order statistics can be computed from the APD. The detector summary analysis computes the following detector values from APDs measured in various bandwidths: peak, RMS, average voltage, and average logarithm. In some EMI receivers and newer spectrum analyzers these statistics are made available by hardware detectors or real-time digitizer/signal processors designed to process the IF signal in comparable ways. The quasi-peak detectors specified by the FCC for most Part 15 measurements below 1 GHz cannot be computed from the APD, because quasi-peak measurements are a function of second-order statistics, as well as first-order statistics.

8.2.10. FCC Proposed Part 15 Measurement Procedures

The FCC suggested in the UWB NPRM that UWB devices be measured according to the existing Part 15.35 (b) measurement techniques referred to in Part 15.209. These measurement techniques include quasi-peak detectors for frequencies below 1 GHz and a pair of measurements (average and peak) for frequencies above 1 GHz. For frequencies above 1 GHz, the FCC specifies in 15.35 (b) that measurements shall be made using an "average detector function." It also states that a maximum peak UWB value should be no more than 20 dB above the average limits, and that (unless otherwise specified) measurements should be made with a minimum bandwidth of 1 MHz. Based on this text, we believe that the FCC has described a Part 15 average detector function corresponding to the average voltage value computed from the 1-MHz APD.

However, the FCC has proposed in their NPRM (Question #50) that Part 15 average measurements be made with a spectrum analyzer using 1-MHz bandwidth, video filtering (between 10-kHz and 10-Hz bandwidth) and a peak detector. No guidance is given in the NPRM

concerning whether logarithmic or linear IF compression is to be used.² It is likely that the use of a logarithmic IF amplifier would give a result very similar to the average logarithm value computed from the 1-MHz APD. If a linear IF were used instead of a logarithmic IF, the result should be very similar to the average voltage value computed from the 1-MHz APD. To confirm this possibility, we also performed an independent measurement that followed the FCC procedures exactly, using a 1-MHz bandwidth, logarithmic IF mode, video filtering, and sample detector. The function of the FCC peak detector is duplicated by manually reading the highest value from the resulting graph. This modified procedure makes it possible to understand the role of sufficient lowpass video filtering in the suggested FCC measurement. This result is labeled "FCC Part 15" and represented by a hollow square in the detector summary graphs.

Detector functions corresponding to peak, RMS, average voltage, and average logarithm have been computed from the APDs measured in each bandwidth and plotted at the corresponding bandwidth for Device D in Figure 8.8. Details on this computation are included in the discussion of APDs in Appendix A. These four detector functions tend to emphasize particular parts of the APD. The peak detector looks only at the single highest measurement value, ignoring all other measurement values. The RMS detector performs an integration of average power. Because power is related to "voltage-squared," the effect of the higher amplitudes in the APD is enhanced. The average voltage detector tends to be affected more equally by the whole range of values. The average logarithm detector gives greatest weight to the lower values. The detectors are normalized to give the same value for a CW signal.

Some common "rules-of-thumb" for these detectors (which should be tested against the detector values actually obtained) include:

1. For Gaussian noise, the peak detector value is typically 8-11 dB greater than the RMS value (depending on the number of samples), the average voltage is 1 dB less than the RMS value, and the average logarithm is 2.5 dB less than the RMS value. The RMS value is exceeded 37% of the time.
2. For non-overlapping pulses, the peak value varies as $20 \log_{10} B$.
3. The RMS value varies as $10 \log_{10} B$.
4. Peak \geq RMS \geq average voltage \geq average logarithm.

Figure 8.8 shows the detector summary graph for Device D, 1-MHz PRR, 100% gating. Dashed lines have been drawn on the graph, corresponding to $10 \log_{10} B$ and $20 \log_{10} B$ slopes. These lines are intended as graphical aids, not as suggested conclusions.

²In a separate communique related to the NTIA UWB test plan, the FCC indicated that the intention was to employ the spectrum analyzer in the logarithmic IF mode.

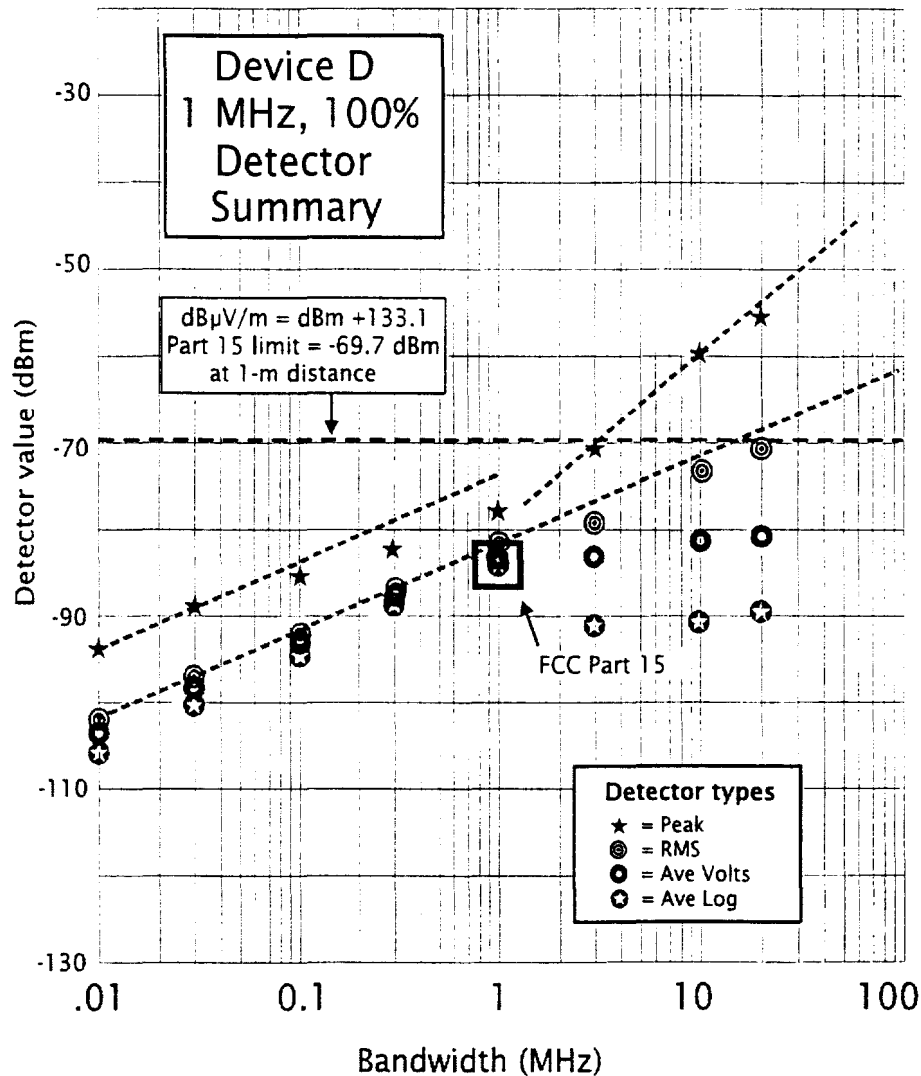


Figure 8.8. Device D detector summary, 1-MHz PRR, 100% gating.

The detector summary shows two major regions: the impulsive region ($B \gg \text{PRR}$) and the noise-like region ($B \ll \text{PRR}$). In the noise-like region, the values for the RMS, average voltage, and average log detectors are closely spaced (2.5 dB theoretical difference between average log and RMS for Gaussian noise). The peak reading is about 8 dB above the RMS (the peak value is theoretically 8-11 dB above the RMS value for Gaussian noise). The values for all detectors change according to a $10 \log_{10} B$ trend. The similarity between the Device D detector readings and the corresponding readings that would have been theoretically produced by Gaussian noise suggest that the Device D signal dithering was selected to make it look similar to Gaussian noise.

A completely different pattern of detector function values is found in the impulsive region ($B \gg \text{PRR}$). There is a much wider divergence between various detector values at any single bandwidth, and this divergence becomes greater as the bandwidth increases. The peak values follow a $20 \log_{10} B$ trend line, and the RMS values follow a $10 \log_{10} B$ trend line. The value of the average voltage and average log detectors drop substantially when the wider bandwidths allow low amplitudes associated with measurement system noise to be seen between the duration of UWB impulses. Since the average log value emphasizes the lowest amplitude signals, the average logarithm value is most dramatically affected when the IF output drops to the measurement system noise level between impulses. The difference between peak values and average logarithm values is as much as 35 dB for the 20-MHz bandwidth. These relatively large differences between detector values suggest that the detector functions used in measuring Part 15 regulatory limits must be specified unambiguously.

The smallest differences between the various detector functions is often seen when $B = \text{PRR}$. In this example, there is only a 6-dB difference between average logarithm and peak values for the 1-MHz values.

The FCC-proposed Part 15 measurement procedure using a spectrum analyzer with 1-MHz bandwidth, logarithmic IF, video filtering, and peak detection was used to make a direct measurement of the Device D signal. This measurement produced a value of about -84 dBm, which was essentially identical to the average logarithm detector value computed from the 1-MHz bandwidth APD.

In addition to the dBm scale on the detector summary graphs, a level has been marked with a horizontal dashed line. This level corresponds to the FCC Part 15 limits from 15.209, which is specified as $500 \mu\text{V/m}$ at a distance of 3 meters. Since all of the measurements in this section of the report were measured at a distance of 1 meter, the FCC limit has been adjusted for a 1-m distance and the gain of the antenna used for the measurement. More details on this conversion can be found in Appendix C.

8.3 Measured Data Summaries for Devices

The following sections contain compilations of measured data from UWB devices A-E and an electric drill. Additional measured data on each device is contained in a corresponding separate section in Appendix D.

8.3.1 Summary of Device A Measurements

Device description. Device A uses a 10-kHz PRR, apparently not gated, dithered, or modulated. ITS had no information on the operational aspects of this device, and testing proceeded on the assumption that the on-off switch was the only significant test variable.

Full bandwidth pulse shape. Figure 8.9 shows a complex pulse shape with multiple lobes, probably caused by a multipole sharp-cutoff RF filter giving a tightly-defined UWB spectrum.

FFT emission spectrum. Figure 8.10 shows most UWB energy is in the 5100-6100 MHz band.

Narrowband peak emission spectra. Spectrum analyzer measurements (Figure 8.11) show most energy in the 5100-6100 MHz range. This spectra had 5-6 irregular lobes about 250 MHz wide, with 10-20 dB nulls between them.

Spectrum fine-structure. Figure 8-12 shows details near 5700 MHz reflecting the 10-kHz PRR of Device A .

Bandwidth progression staircase. Figure 8-13 clearly shows 10-dB steps for bandwidths greater than the 10-kHz PRR (impulsive behavior) and 5-dB steps (noise-like behavior) for bandwidths less than 10 KHz .

APDs. Figure 8-14 shows impulsive behavior for all measurement bandwidths greater than 10 kHz. However, although the peak values followed a $20 \log_{10} B$ trend line for the narrower bandwidths, the 1-MHz and 3-MHz peak values (Figure 8.15) were appreciably lower than the trend line (8 dB lower at the 3-MHz bandwidth). This 8-dB difference was traced to a deficient component in the spectrum analyzer, which was found to provide insufficient spectrum analyzer video bandwidth and was replaced by the manufacturer. Unfortunately, Device A had already been returned to its owner when the repaired spectrum analyzer became available. It should probably be assumed that a re-measurement of Device A would have placed the 1-MHz and 3-MHz readings on the proper trend lines.

Detector summary. We note in Figure 8-15 that the detector values are within 8 dB of each other in the 10-kHz measurement bandwidth, and they diverge rapidly as the bandwidth is increased. The difference between peak and average logarithm is as much 40 dB for the 3-MHz bandwidth (presumably, this difference would have been 8 dB greater – a 48-dB difference – if the spectrum analyzer had been working properly during these measurements).

FCC Part 15 measurement. The FCC-recommended Part 15 measurement procedure (1-MHz bandwidth, logarithmic IF, video filtering, and peak detection) produced a value of -112 dBm with a 300 Hz video bandwidth (300 Hz was the minimum video bandwidth for the spectrum analyzer when used with 1-MHz resolution bandwidth). This matches the -112 dBm average logarithm detector value in Figure 8-15 computed from the 1-MHz bandwidth APD.

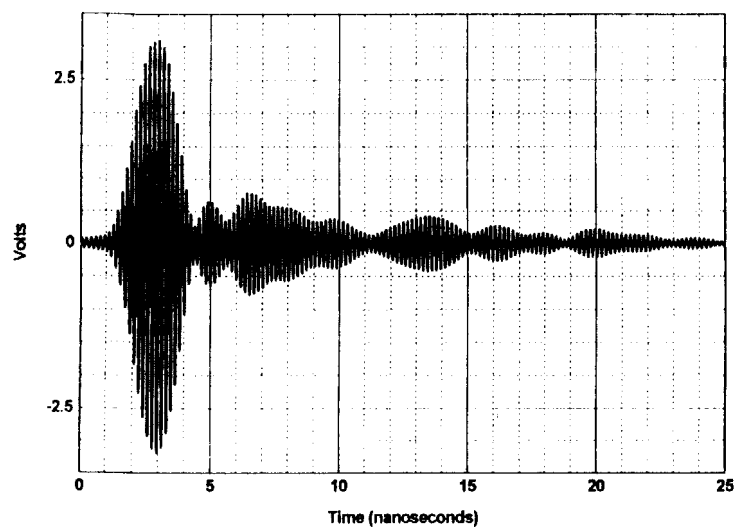


Figure 8.9. Device A full bandwidth pulse shape.

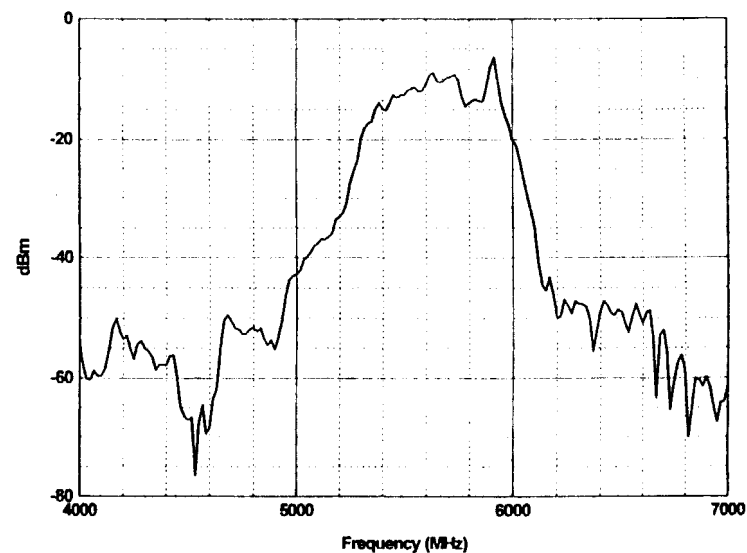


Figure 8.10. Device A, conducted power spectrum, $\Delta f = 16.67$ MHz.

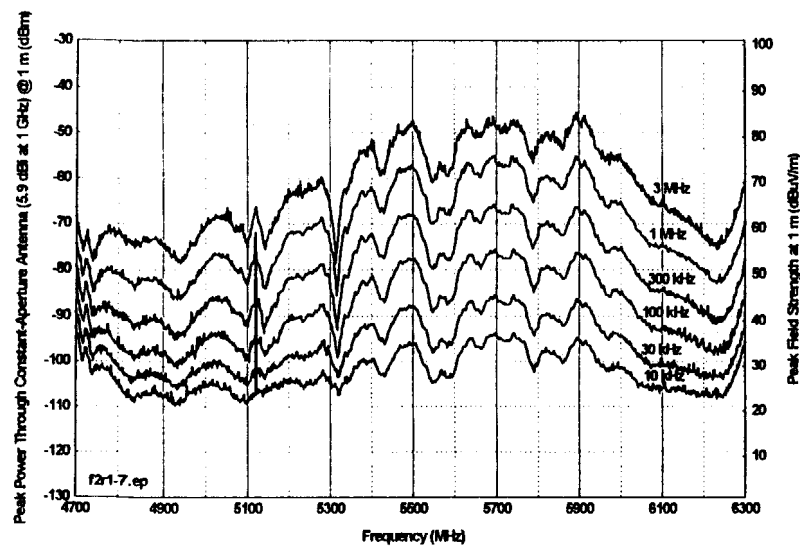


Figure 8.11. Device A spectra as a function of measurement bandwidth.

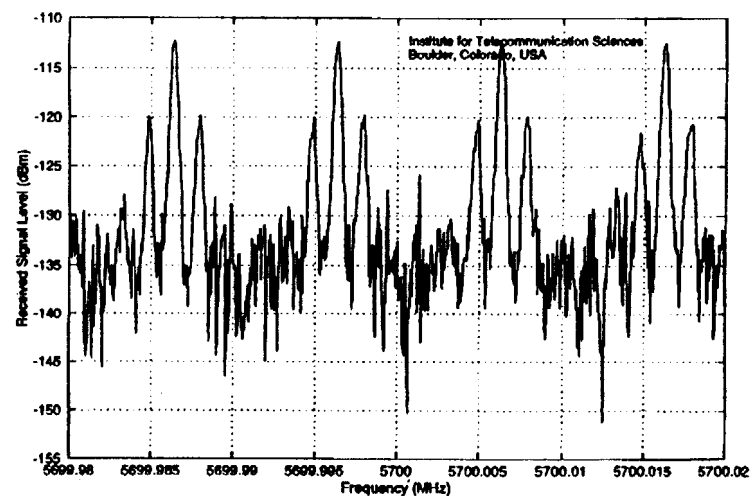


Figure 8.12. Device A spectrum fine structure.

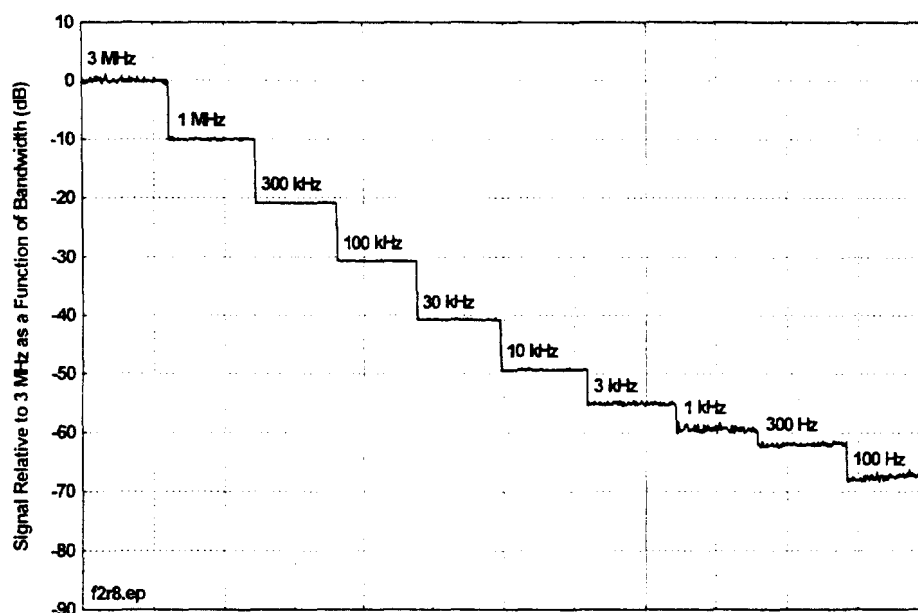


Figure 8.13. Device A peak amplitude as a function of bandwidth.

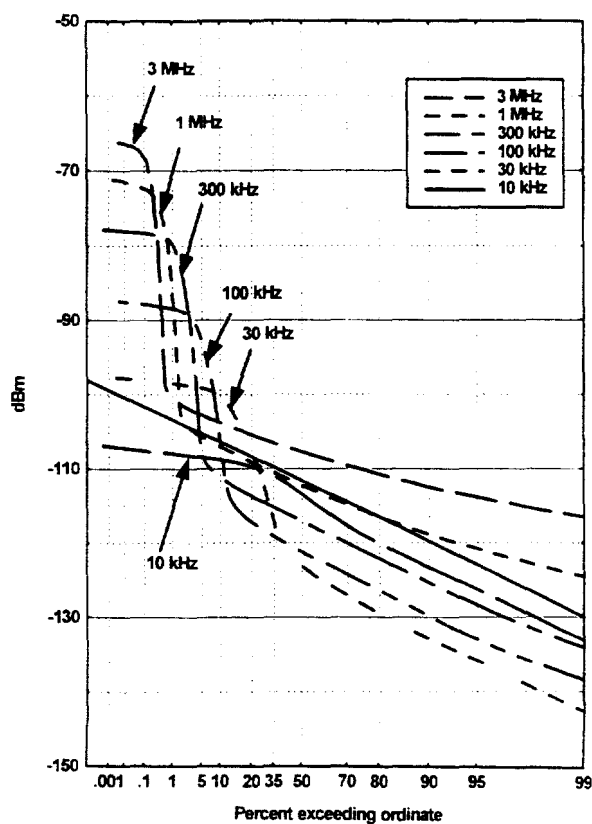


Figure 8.14. Device A APDs.

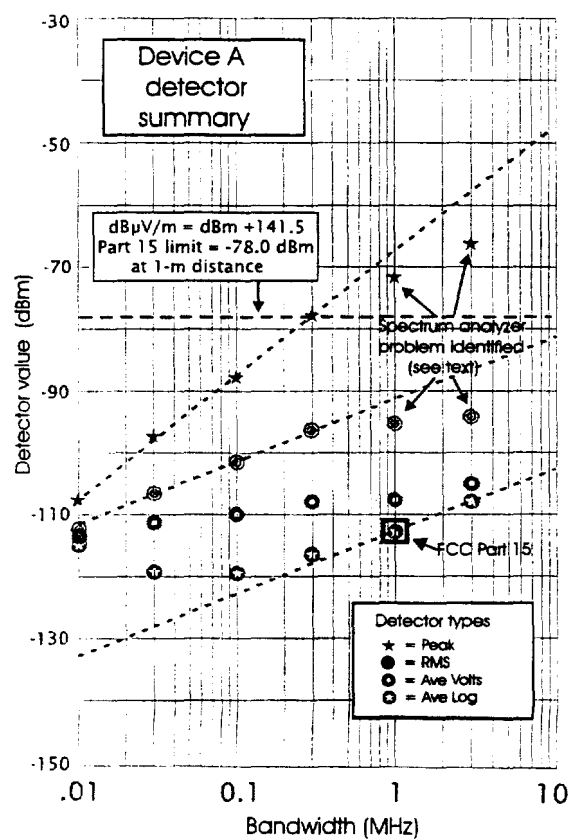


Figure 8.15. Device A detector summary.

8.3.2 Summary of Device B Measurements

Device description. Device B operates in four data rate modes, ranging between 16 kb/s and 128 kb/s. Any of these data rates can be used to support a two-way voice circuit or a two-way data circuit. ITS measured the device in its 16-kb/s and 128-kb/s voice modes, but did not measure the intermediate 32-kb/s and 64-kb/s modes.

The 16-kb/s mode provides an average user data rate of 16 kb/s, using a transmitted signal of about 100 K impulses per second, which is gated on for 8.8 ms and gated off for 35.2 ms (44 ms total cycle time). During the 8.8 ms when the signal is gated on, the data stream is modulated on the train of impulses by deleting selected pulses (on-off keying). Corresponding gating and PRR values for the other modes can be found in Table 8.1.

Table 8.1. Burst and PRR Timing for Various Data Rates

Data Rate (kb/s)	Burst length (on time, ms)	Burst Repetition time (ms)	Burst duty cycle (gating)	Pulse repeti- tion rate (PRR)
16	8.8	44	20%	100 kHz
32	4.4	22	20%	200 kHz
64	2.2	11	20%	400 kHz
128	2.2	5.5	40%	400 kHz

Full bandwidth pulse shape. Device B emission spectrum is tightly filtered to limit it to a 500 MHz-wide bandwidth. This filtering produces relatively complex and extended pulse shapes, lasting up to 30-40 ns (Figure 8.16).

FFT emission spectrum. The FFT-derived spectrum (Figure 8.17) shows a sharply-defined 500-MHz RF bandwidth. The peak signal in the FFT-derived spectrum is 116 dB μ V/m in a bandwidth, Δf , equal to 20 MHz.

Narrowband peak emission spectra. Figures 8.18 and 8.19 show a sharply-defined bandwidth between 1250 and 1800 MHz, with 5-6 ripples of 5-10 dB depth across the passband. The peak signal measured with a spectrum analyzer in a 3-MHz bandwidth (Figures 8.1 or 8.19) is approximately 100 dB μ V/m. Since the UWB signal for Device B is impulsive at bandwidths greater than the PRR (maximum PRR = 400 kHz) a $20 \log_{10} B_1/B_2$ correction factor is needed to convert the 3-MHz bandwidth data to 20-MHz data. This correction factor equals 16.5 dB. This converts the 3-MHz bandwidth value measured by the spectrum analyzer to the corresponding 20-MHz bandwidth value of 116.5 dB μ V/m, which compares closely with the FFT-computed value of 116 dB μ V/m.

Bandwidth progression staircase. The stair step bandwidth progression figures (Figures 8.20 and 8.21) suggest that Device B produces signals that appear noise-like for measurement bandwidths less than the 100-kHz or 400-kHz PRR's associated with the respective 16-kb/s and 128-kb/s modes, made at 1325 MHz and 1500 MHz respectively.

Gating, PRR, and modulation. Figures 8.22 and 8.23 show the 20% and 40% gating duty cycles for the 16-kb/s and 128-kb/s modes, respectively. Figures 8.24 and 8.25 show the basic PRRs for the 16-kb/s and 128-kb/s modes, respectively. Figure 8.26 shows an example of a missing pulse, caused by the on-off pulse modulation of the Device B data stream.

APDs. Both APDs (Figures 8.28 and 8.29) were measured at 1545 MHz. These APDs were inadvertently measured using video filtering equal to the resolution bandwidth, which prevented the low-amplitude portion of the APD from reaching minimum values. This effect is believed to have prevented this portion of the APDs from following the expected straight line. This problem was recognized and corrected in subsequent APD measurements for other devices. The very steep sides on the "plateau" at 20% and 40% respectively for the 16-kb/s and 128-kb/s modes reflect the respective 20% and 40% gating modes.

Detector summaries. The detector summaries (Figures 8.30 and 8.31) show approximately a 30-dB difference between peak and average logarithm and a 20-dB difference between average logarithm and RMS values for the narrower bandwidths, caused mainly by the gating modes. During the gated-off period, system noise is the only signal contributing to the APD. Since the average logarithm value is affected most by low amplitude, high-percentage signals, measurement system noise has a strong effect on the average logarithm value of gated signals.

The peak value follows a $10 \log_{10} B$ trend line (like Gaussian noise) for bandwidths less than the PRR and a $20 \log_{10} B$ trend (like an impulse) for bandwidths greater than the PRR. Peak measurements are identical for both 3-MHz bandwidth APDs, where impulses are non-overlapping. For the lower bandwidths where the signal acts like Gaussian noise, peak measurements for each PRR differ by about 6 dB, which would be expected from the 4:1 ratio in the number of pulses/s (not counting the percentage gating ratio).

The RMS values follow a $10 \log_{10} B$ line for all bandwidths. The best-fit trend lines for the two modes are about 8 dB apart. A difference of 9 dB would have been expected, based on the 8:1 ratio in the total number of impulses (including the effect of the 2:1 change in gating ratio).

FCC Part 15 measurement. A measurement similar to the Part 15 measurement (except using a 3-MHz bandwidth) was done at 1650 MHz, 128 kb/s mode with logarithmic IF, 10-Hz video bandwidth, and sample detection (Figure 8.27). This gave an maximum measurement of about -74.5 dBm, with less than 1-dB time ripple caused by the 5.5 ms gating cycle. Compensating for the gain of the 19 dB preamplifier, the "Part 15-like" value was -93.5 dBm, which is within 2 dB of the average logarithm computed from the 3-MHz APD. No Part 15 measurements were made at 1-MHz bandwidth or using the 16-kb/s mode.